membered ring which involves both carbons of ethylene, the hydrogen molecule, the oxygen or fluorine atom, and the acidic proton. Several common points have to be stressed: a proton must be transferred from the acid toward ethylene; the hydrogen molecule breaks and forms a hydride ion, and a proton is subsequently formed to generate the initial acid molecule. However, differences between a normal acid and a strong acid arise in reactions 2 and 3. In (2), catalyzed by HF, there is a bifunctional catalysis and the process is very concerted. The acid acts as a catalyst that simultaneously releases and accepts a proton. In this way, the acid contributes to the breakage of the hydrogen molecule. Similar bifunctional catalysis have been theoretically studied and reported in the literature for analogous processes.[28] In contrast to (2), in reaction 3, catalyzed by a strong acid such as H_3O^+, the first phase of the process consists of the full proton transfer from the acid to ethylene to form the carbocation. Not until a second phase is the hydrogen molecule broken owing to the action of the existing carbocation, helped by the conjugated base of the acid. This mechanism is almost coincident with the mechanism proposed from experimental data, where a carbocation is formed in a first step, and a hydride ion attacks later the carbocation to form the alkane.[8a] Our mechanism for reaction 3 is distinguished from the experimentally proposed mechanism in that, although a carbocation is formed initially, the mechanism does not proceed through two steps but via an unique step with two phases.

If we compare the acid catalysis as described in this paper with the heterogeneous or homogeneous catalysis by metals, a remarkable difference exists. Whereas metal catalysis implies breakage of the hydrogen molecule as a first step, the acid catalysis in reaction 3 requires the formation of the carbocation in the first phase. The catalysis by normal acids such as HF (eq 2) exhibits an intermediate behavior, because the hydrogen molecule rupture and the carbocation formation are simultaneously done, as seen in the concertedness of the reaction.

A last aspect of the two acid-catalyzed reactions studied in this paper is their possibility of being carried out experimentally. With respect to the catalysis by hydrogen fluoride, it is clear that it implies a high internal energy barrier that will make the actual reaction quite difficult. Furthermore, a competitive reaction exists that involves entrance of HF instead of H_2 into ethylene and proceeds via a lower energy barrier.[29] Finally, the reactant complexes $C_2H_4 \cdot HF$ and $C_2H_4 \cdot HF \cdot H_2$ have $\Delta G^\circ_{298} > 0$, so that their population with respect to separated species will be minimal. On the contrary, catalysis of ethylene hydrogenation by H_3O^+ seems to be very favorable from either, the low computed energy barrier and the free-energy stability of the reactant complex $C_2H_4 \cdot H_3O^+ \cdot H_2$. This complex can be easily generated by a collision of the very favorable complex $C_2H_4 \cdot H_3O^+$ and a hydrogen molecule. It is clear that other reactions like the acid-catalyzed formation of alcohols may compete with hydrogenation, but certain experimental conditions may be chosen so that hydrogenation becomes the main reaction.

Conclusions

In the present work we have theoretically studied the acid catalysis of olefin hydrogenation reactions. Ethylene has been chosen as a model for olefin, while HF and H_3O^+ have been chosen as models for normal and strong acids, respectively. Whereas catalysis by a normal acid shows bifunctional characteristics and does not seem to be very efficient, catalysis by a strong acid exhibits special characteristics such that, given an adequate choice of experimental conditions, it may be an adequate way to hydrogenate olefins. Existing experimental data on the acid-catalyzed hydrogenation of aromatic compounds show the feasibility of this type of reactions, which in our opinion are worth further experimental research effort.

Acknowledgment. This work has been supported by the Spanish "Comisión Asesora de Investigación Cientifica y Técnica" under Contract No. 3344/83.

Registry No. $CH_2{=}CH_2$, 74-85-1; HF, 7664-39-3; H_3O^+, 13968-08-6.

(28) (a) Ruelle, P.; Kesselring, U. W.; Nam-Tram, H. *J. Am. Chem. Soc.* **1986**, *108*, 371-375. (b) Clavero, C.; Duran, M.; Lledós, A.; Ventura, O. N.; Bertrán, J. *Ibid.* **1986**, *108*, 923-928.

(29) Kato, S.; Morokuma, K. *J. Chem. Phys.* **1980**, *73*, 3900-3914.

Theoretical Calculations on Adenine and Adenosine and Their 8-Chloro-Substituted Analogues

Gerald A. Walker,[†,‡] Subhash C. Bhatia,[‡] and John H. Hall, Jr.*[‡,⊥]

Contribution from the Department of Chemistry, Atlanta University, Atlanta, Georgia 30314, Dolphus E. Milligan Science Research Institute, Atlanta University Center Inc., Atlanta, Georgia 30310, and the School of Geophysical Sciences, Georgia Institute of Technology, Atlanta, Georgia 30332. *Received March 26, 1987*

Abstract: Ab initio STO-3G level calculations and localized molecular orbitals from the partial retention of diatomic differential overlap method are reported for various protonated and tautomeric forms of adenine. The localized molecular orbitals indicate that the bonding patterns of the electrons are highly sensitive to the protonated site, consistent with experimental results. Calculation of the conformational energies of adenosine shows that N_3-protonation is more favorable in the anti conformation than N_3 protonation in the syn conformation by 32.2 kcal/mol. Our calculations also indicate that N_3-protonation may cause a change in conformation. The calculations for 8-chloroadenosine show a higher rotational barrier about the base-ribose bond than the rotational barriers obtained for adenosine and N_3-protonated adenosine.

Many different approaches[1] have been used to determine the underlying mechanisms related to the function of DNA and RNA in biological systems. One approach has been to examine the chemistry of their basic units in relation to the behavior of the macromolecular structures in attempts to explain the experimental data.[2] Since it is extremely difficult to experimentally determine the atomic interactions in enzymes and macromolecular systems, theoretical techniques have been very useful for studying reaction mechanisms in biological systems.[3]

[†] Atlanta University.
[‡] Atlanta University Center Inc.
[⊥] Georgia Institute of Technology.

(1) Saenger, W. *Principles of Nucleic Acid Structure*; Springer-Verlag: New York, 1974; Chapter 3.
(2) Reference 1; Chapter 1.

0002-7863/87/1509-7629$01.50/0

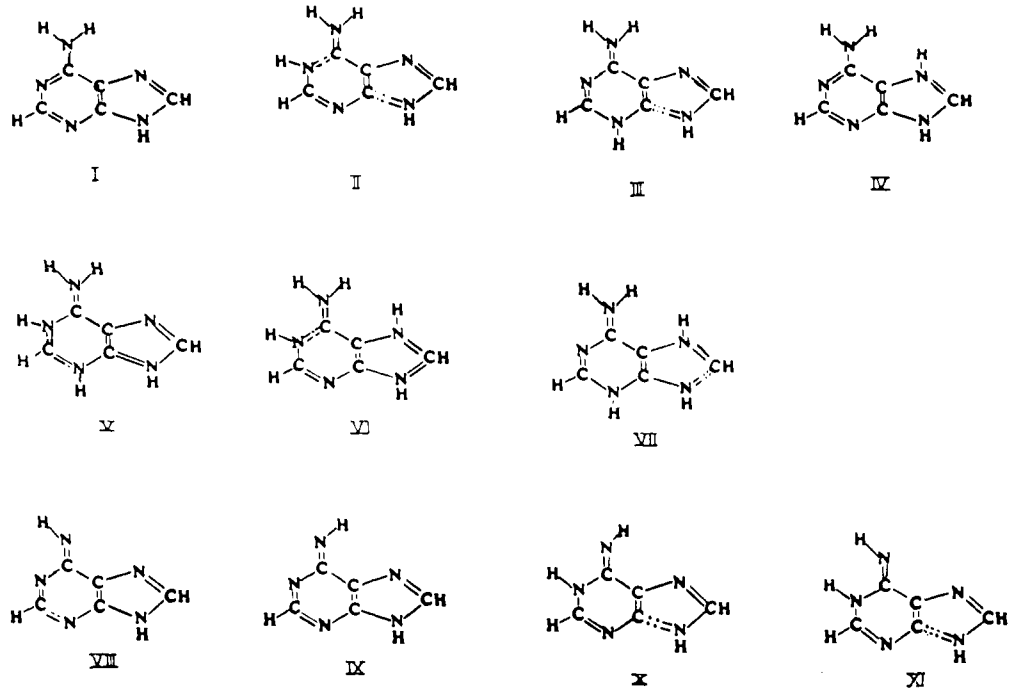

Figure 1. Various protonated and tautomeric forms of adenine.

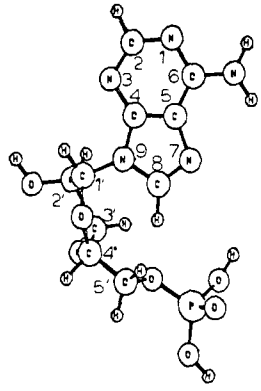

Figure 2. Adenosine-5′-monophosphate; anti conformation.

The keto–enol tautomerism in guanine is believed to play an important role in the mechanism for the initiation reaction of the "cap" of messenger ribonucleic acid (mRNA) because the reaction rate is a function of pH of the solution.[4] The tautomeric forms of the nucleic acid bases are also believed to play a role in causing mutations.[5a] These tautomers can hydrogen bond with other bases to form base pairing schemes that do not conform to the normal Watson–Crick base-pairing scheme.[5a] In these rare tautomeric forms, adenine can pair with cytosine, guanine, or adenine; and guanine can pair with thymine, uracil, or adenine.[5a] This mispairing of the nucleic acid bases, which is sometimes accompanied by a change in the base–ribose conformation, can give rise to mutations.[5a] The helix formed by the mispaired base is similar to that of the normal helix structure so the checking enzymes do not detect the misplaced tautomer. In the codon–anticodon relationship, mispairing of bases due to the presence of a rare tautomeric form can occur in the "wobble" position,[6] leading to placement of the wrong amino acid residue in protein synthesis.[5b] Atomic and molecular substitution on the rings of the nucleic acid base has also been shown to shift the tautomeric equilibria of nucleic acid bases.[6] The role of substituted nucleotides in biopolymers has not been determined, but the majority of naturally occurring modified nucleotides have been found in transfer RNA (tRNA).[7] Substituted nucleotides[8] have been extensively used in studies on enzyme activity in a "trial and error" method for studying the effectiveness of a new compound as an antiviral or anticancer agent[9] and as biological probes in mechanistic studies.[10a] Some encouraging results in the treatment of AIDS and AIDS related complexes have been produced with a ribose-substituted nucleoside 3′-azido-3′-deoxythymidine (AZT).[10b]

The pH-dependent laser Raman spectra of 5′AMP and 8-Br-5′AMP indicate that N_3-protonation is influenced by the conformation of the molecule.[11] These results[11] also indicate the possibility of the presence of various tautomeric forms. Szczepaniak et al.[12] performed ab initio self-consistent-field (SCF) calculations on the tautomers of guanine to determine the most stable tautomeric form. This study reports ab initio SCF calculations for various protonated forms of adenine. Conformational energy calculations are performed for adenosine, and N_3-protonated adenosine, in order to examine the effect of conformation on N_3-protonation. The results of the conformational energy calculations for 8-chloroadenosine are also reported.

Method

The electronic energy calculations were performed on structures I to XI (Figure 1). The optimized geometries for forms I, II, III IV, and

(3) (a) Pincus, M. R.; Scheraga, H. A. *Acc. Chem. Res.* **1981**, *14*, 299. (b) Sheiner, S. *Acc. Chem. Res.* **1985**, *18*, 174. (c) Menger, F. M. *Acc. Chem. Res.* **1985**, *18*, 128. (d) Lipscomb, W. N. *Acc. Chem. Res.* **1982**, *15*, 232. (e) Dewar, M. J. S.; Storch, D. M. *Proc. Natl. Acad. Sci. U.S.A.* **1985**, *82*, 2225.

(4) Rhoads, R. E.; Hellman, G. M.; Remy, P.; Ebel, J. P. *Biochemistry* **1983**, *22*, 6048.

(5) (a) Topal, M. D.; Fresco, J. R. *Nature (London)* **1976**, *263*, 285. (b) Topal, M. D.; Fresco, J. R. *Nature (London)* **1976**, *263*, 289.

(6) Hillen, W.; Egert, E.; Linder, H. J.; Gassen, H. G.; Vorbruggen, H. *J. Carbohydr. Nucleosides, Nucleotides* **1978**, *5(1)*, 23. Brown, D. M.; Hewlins, M. J. E.; Schell, P. *J. Chem. Soc. C* **1968**, 1925–1929.

(7) Agris, P. F. *The Modified Nucleosides of Transfer RNA*; A. R. Liss: New York, 1980.

(8) (a) Hall, R. H. *The Modified Nucleosides in Nucleic Acids*; Columbia University Press: New York, 1971. (b) Reference 1; Chapter 7.

(9) (a) *Nucleoside Analogues, Chemistry, Biology, and Medical Applications*; Walker, R. T., De Clercq, E., Eckstein, F., Eds.; Plenum: New York, 1979. (b) Suhadolnik, R. J. *Nucleoside Antibiotics*; Wiley: New York, 1970.

(10) (a) Suhadolnik, R. J. *Nucleosides as Biological Probes*; Wiley: New York, 1979. (b) Dagan, R. *Chem. Eng. News* **1986**, *Dec. 8*, 7.

(11) Walker, G. A. M.S. Thesis, Atlanta University, Atlanta, GA, May 1986, Chapter I. Walker, G. A.; Bhatia, S. C.; Hall, J. H., Jr. *J. Am. Chem. Soc.*, following paper in this issue.

(12) (a) Szczepaniak, K.; Latajka, Z.; Morokuma, K.; Person, W. B., Presented at the Vth International Conference on the Spectroscopy of Matrix Isolated Species, Abbaye de Fontevraud, France, June 8–12, 1985. (b) Jones, P.; Bhatia, S. C.; Hall, J. H., Jr., unpublished results.

Table I. Electronic Energies[a] of Various Protonated and Tautomeric Forms of Adenine

structure	STO-3G	PRDDO
I	−458.621 50	−463.417 73
II	−459.081 27	−463.856 69
III	−459.074 59	−463.849 06
IV	−459.056 89	−463.829 66
V	−459.322 86	−464.080 91
VI	−459.341 94	−464.094 60
VII	−459.335 88	−464.088 78
VIII	−457.877 21	−462.702 72
IX	−457.874 99	−462.701 55
X	−458.573 67	−463.374 39
XI	−458.563 42	−463.372 93

[a] Energies in au.

VIII–XI were taken from Del Bene's protonation study of nucleic acid bases.[13] In that study,[13] the geometries for adenine and singly protonated adenines were optimized with an STO-3G basis set with the GAUSS80 program. The geometries for the doubly protonated forms (V, VI, and VII) were estimated from the geometries of II, III, and IV. In order to estimate the geometries for V, VI, and VII, the difference in the bond lengths of II, III, or IV were calculated, and the new bond lengths were determined on the basis of the magnitude of the difference, the direction of the difference, and the location of the bond with respect to the protonated site. For example, the geometry for V was estimated from the geometries of structures II and III, but the geometry for VI was estimated from the geometries of structures II and IV. The geometries used for structures V, VI, and VII are available upon request. The C_8–Cl, N_9C_8, N_7C_5, N_7C_8, and N_9H bond lengths of 8-chloroadenine were optimized at the STO-3G level with the GAUSS80 program.

The localized molecular orbitals (LMOs) were calculated from wave functions from the partial retention of diatomic differential overlap (PRDDO) method[14] by using the Boys' criterion,[15] which maximizes the orbital centroid distances for determining the LMOs. The criterion for partial bond formation are those described by Kleier and Lipscomb.[16] LMO centers having an electron population density (EPD) of <0.35 e are not considered as bonding. Those LMO centers having 0.35–0.60 e are drawn as half dotted–half solid lines, while those having EPD > 0.60 e are drawn as solid lines.

Ab initio calculations were performed with the GAUSS80 program (QCPE No. 446).[17] The calculations of the electronic energies employed STO-3G basis sets.[18] The torsion angle used for varying the conformation about the base–ribose bond involves the C_8, N_9, C_1', and O in the ribose ring (Figure 2). The conformation of the ribose ring has been shown to be dependent on the conformation of the base relative to the ribose moiety.[19] The conformation of the ribose ring was held fixed for all of the base–ribose conformations. The ribose geometry used in these calculations is taken from Saenger.[20]

Protonation energies were calculated by subtracting the SCF energies of the reactants from the energies of the products.

Results and Discussion

Protonation and Tautomerization Energies. The electronic energies for structures I through XI are presented in Table I. The relative ordering of the energies of the singly protonated species is calculated to be $N_1 < N_3 < N_7$. The protonation energy (Table II) for the N_7 site is −101.9 kcal/mol, that for N_3 is −113.1 kcal/mol, while the N_1-protonation energy is −117.2 kcal/mol. Since the difference in energy between N_1- and N_3-protonation is calculated to be 4.1 kcal/mol, it is expected that a hydrogen exchange may take place between N_1 and N_3 in acidic solution.[11] The N_7 site, which is also important in metal–ion interactions, is reported to be protonated at very low pH values; thus, the calculated order of protonation is in good agreement with the reported pK_a values for the N_1 and N_7 sites.[21]

Table II. Protonation Energies[a] of Adenine

protonation site	energy (kcal/mol)	protonation site	energy (kcal/mol)
N_1	−117.2	N_1 and N_7	−109.5
N_3	−113.1	N_1 then N_7[b]	7.9
N_7	−101.9	N_7 then N_1[b]	−7.6
N_1 then N_3[b]	19.7	VIII[c]	295.8
N_3 then N_1[b]	15.5	X[d]	30.0
N_1 and N_3	−97.6	X[e]	27.2
N_3 and N_7	−105.7		

[a] $H^+ + A \rightarrow HA^+$. [b] N_x then N_y = order of protonation: first N_x is protonated then N_y is protonated. Value listed is for N_y protonation. [c] Deprotonation energy. [d] Tautomerization energy (STO·3G). [e] Tautomerization energy (PRDDO).

The relative energy ordering for the doubly protonated species is calculated to be $N_1N_7 < N_3N_7 < N_1N_3$ (Table I). Crystallographic data indicate the presence of a doubly protonated species involving the N_1 and N_7 sites.[22] Our calculations also predict this form to be the most stable doubly protonated species (Table I), with a protonation energy of −109.5 kcal/mol (Table II).

When the order of protonation is N_1 and then N_7, the protonation energy for the second step of the reaction is calculated to be 7.69 kcal/mol; however, when the order of protonation is N_7 then N_1 the protonation energy for the second step of the reaction is calculated as −7.61 kcal/mol. These results also suggest that an N_7 singly protonated species may not exist.

When the doubly protonated species V (Figure 1) is generated by protonating N_1 then N_3, the protonation energy for the second protonation step is 19.7 kcal/mol. If the order of protonation is N_3 then N_1, the protonation energy for the second protonation is 15.5 kcal/mol. In this approximation, these relative protonation energies indicate that it is easier to protonate N_1 when N_3 is protonated than it is to protonate N_3 when N_1 is protonated. This observation is consistent with the nuclear magnetic resonance study of Sarma et al.,[19] which indicates that the hydrogen bond between the N_3 position of 8-bromoadenosine and the 5′OH of adenosine is weakened when N_1 is protonated.

The localized molecular orbitals (Figure 1) show that when N_1 is protonated (II, VI) a partial double bond ($0.35 < e < 0.60$) exists between N_1 and C_6 but when N_3 is protonated (III, V, VII) the partial (V) or full (III, VII) double bond is between N_1 and C_2. The theoretical results are in agreement with our experimental data,[11] which suggest that the changes observed in the 1456- and 1578-cm^{-1} absorptions of 8-Br-5′AMP and the 1483- and 1580-cm^{-1} absorptions of 5′AMP are due to protonation at different sites and that those sites seem to play a major role in determining the positions of the double bonds inside the rings of the base.

The PRDDO calculations on the N_7-protonated species give an energy difference of 12.5 kcal/mol in total energy between the N_3- and N_7-protonated species. This result is in close agreement with the STO-3G basis set calculations (11.2 kcal/mol).

According to the criterion developed by Kleier and Lipscomb[16] for determining partial or full bond formation, structures V, VI, VIII, and IX are predicted to have five bonds at various carbon atoms (Figure 1). A pentabonded carbon has been previously predicted for the methanium ion[23a,b] and in alkyllithium clusters.[23c] These compounds contain three-center two-electron bonds with C_s symmetry, the carbon has a positive charge, and the sum of electrons around this center is 6.7 e with the remaining electron

(13) Del Bene, J. E. *J. Phys. Chem.* **1983**, *87*, 367.
(14) Halgren, T. A.; Lipscomb, W. N. *J. Chem. Phys.* **1973**, *58*, 1569.
(15) (a) Boys, S. F. *Rev. Mod. Phys.* **1960**, *32*, 306. (b) Foster, J. M.; Boys, S. F. *Rev. Mod. Phys.* **1960**, *32*, 300. (c) Boys, S. F. *Quantum Theory of Atoms, Molecules, and the Solid State*; Per-Olov Lowdin, Ed.; Academic: New York, NY, 1966; p 253.
(16) Kleier, D. A.; Lipscomb, W. N. *Int. J. Quantum Chem.* **1977**, *S4*, 73.
(17) Singh, C.; Kollman, P. *Quantum Chemistry Program Exchange* (QCPE), Program No. 446.
(18) Hehre, W.; Stewart, R.; Pople, J. *J. Chem. Phys.* **1969**, *51*, 2657.
(19) Sarma, R.; Lee, C.; Evans, F.; Yathindra, N.; Sundaralingam, M. *J. Am. Chem. Soc.* **1974**, *96*, 7337.
(20) Saenger, W. *Angew. Chem.* **1973**, *12*, 591.
(21) Beyerle-Pfnur, R.; Brown, B.; Faggiani, R.; Lippert, B.; Lock, C. *Inorg. Chem.* **1985**, *24*, 4001.
(22) (a) Bryan, R. F.; Tomita, K. *Acta Crystallogr.* **1962**, *15*, 1179. (b) Kistenmacher, T. J.; Shigematsu, T. *Acta Crystallogr.* **1974**, *B30*, 1528. (c) Langer, V.; Huml, K. *Acta Crystallogr.* **1978**, *B34*, 1157.
(23) (a) Sefcik, M. D.; Henis, J. M. S.; Gaspar, P. P. *J. Chem. Phys.* **1974**, *61*, 4321. (b) Yamabe, S.; Osamura, Y.; Minato, T. *J. Am. Chem. Soc.* **1980**, *102*, 2268. (c) Graham, G.; Richtsmeier, S.; Dixon, D. *J. Am. Chem. Soc.* **1980**, *102*, 5759.

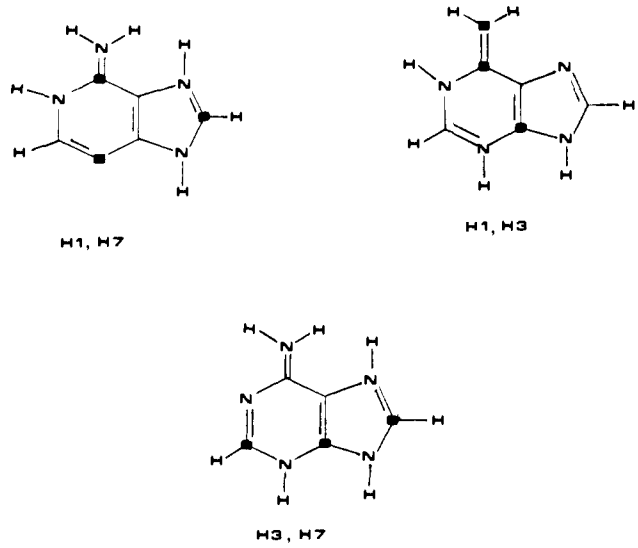

Figure 3. The three largest atomic charge increments for the doubly protonated adenines.

Table III. Relative Conformational Energies of Adenosine, N_3-Protonated Adenosine, and 8-Chloroadenosine

torsion angle[a] (deg)	relative energy (kcal/mol) adenosine	N_3-protonated adenosine	8-chloro-adenosine
0	3.97	2.29	17.00
30	0.0	2.86	1.56
60	16.94		
90			
120			
150	30.87	49.64	
210	2.22	0.0	0.0
270	56.89	59.71	
330	21.29	7.85	

[a] Torsion angle is about the C_8N_9–$C_1'O$ bond (Figure 1).

density between the two hydrogens of the three-center two-electron bond. The PRDDO method gives a sum of electrons surrounding the carbon with five bonds in structure V that is slightly less than the required number of electrons for the valence shell of a carbon atom (3.85 e; ideally the carbon atom valence shell has 4 e, thus the carbon retains a slightly positive charge). The total number of bonding electrons at C_4 for structure V is 9.65 e. The electron density for the bonds that cause five bonds to be drawn to carbon in the doubly protonated species V and VI is just over the limit prescribed by Kleier and Lipscomb[16] at 0.63 and 0.62 e, respectively. Lone-pair donation by N_9 to C_4 occurs for the N_1N_3 doubly protonated species, but for the N_1N_7 doubly protonated species the lone pair on N_9 is donated to C_8. σ bond density rearrangements result in an overall increase in atomic charge for each atom. The sum of all the atomic charge increments equals 2.0 e (in effect the +2 charge has been delocalized). A diagram showing the three atoms giving the largest increment in charge for the doubly protonated species is given in Figure 3. Therefore, the highly charged doubly protonated species is stabilized by rearrangements in σ bond density and polarization of the π electron density. In the negatively charged structures (VIII and IX), the bond between C_2 and N_3 has an electron density of 0.69 e, the number of electrons on atom C_2 is 4.03 e (i.e., it holds a small negative charge), and the total number of bonding electrons surrounding C_2 is 9.53 e. The N_1 and N_6 atoms hold the majority of the negative charge (5.29 and 5.34 e, respectively) due to deprotonation. Thus it seems that the criterion for bonding prescribed by Kleier and Lipscomb[16] for peptides does not adequately predict the bonding patterns for charged heterocycles. Basis set effects[24] may also be a determining factor because the

(24) Mo, O.; G. de Pas, J.; Yanez, M. *J. Phys. Chem.* **1986**, *90*, 5597.

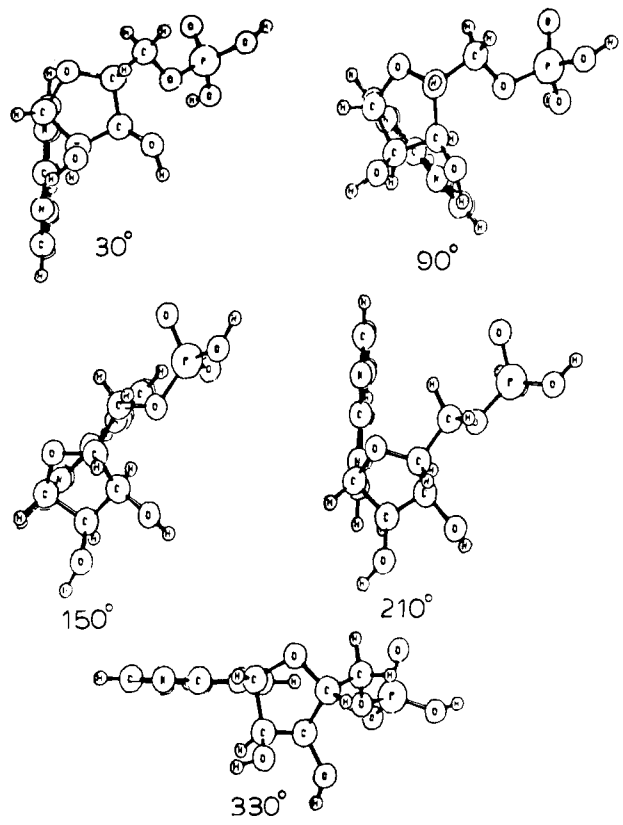

Figure 4. Conformations of 5'AMP at various torsion angles.

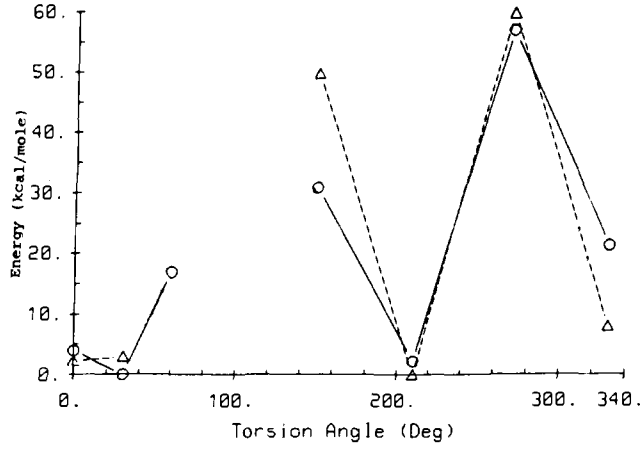

Figure 5. Relative conformational energies for rotation about the base–ribose bond of adenosine.

LMO structures were determined from PRDDO with use of geometries optimized with an STO-3G basis set.

Conformational Energies. The conformational energy results (Table III) show that the rotational barrier for the unprotonated species is lower than the rotational barrier for the N_3-protonated species by 2.82 kcal/mol. The lowest energy conformation for the unprotonated species occurs when the torsion angle is 30°, and the next lowest energy occurs for a torsion angle of 210° (Figure 4). The difference in energy of the syn (210°) and anti (30°) conformations for unprotonated adenosine is 2.19 kcal/mol, and the rotational barrier is 56.89 kcal/mol (Figure 5).

For adenine nucleotides in the anti conformation, the ribose is generally found in the C_2' endo conformation; however, for a syn *N*-glycosyl conformation, the ribose shows only a slight preference for the C_2' endo conformation.[19] The change in ribose conformation can minimize the repulsions between the base and sugar hydrogens for the syn conformation which lowers the overall

Table IV. N_3-Protonation Energies of Adenosine at Various Conformations

torsion angle[a] (deg)	energy (kcal/mol)	torsion angle[a] (deg)	energy (kcal/mol)
0	−129.5	210	−130.6
30	−125.5	270	−125.5
150	109.6	330	−141.8

[a] Torsion angle is about the C_8N_9–$C_1'O$ atoms (Figure 1).

energy. The N–glycosyl bond length is shown to vary with the ribose conformation.[1] If there is a correlation with N–glycosyl torsion and ribose conformation, then N–glycosyl bond length should vary with the torsion angle. However, the N–glycosyl bond length is not influenced by the N–glycosyl torsion angle in purines,[1] thus, no significant change in the overall result is expected from optimization of this bond length. Therefore, this calculation represents an upper bound to the true energy because the ribose conformation was not optimized nor varied with the N–glycosyl torsion angle. The sugar pseudorotation barrier is estimated to be 5 to 6 kcal/mol for furanose.[1] Assuming that the rotational barriers for the N–glycosyl torsion and the ribose pseudorotation are additive, the energy values for the total rotational barrier for this structure should be higher than the values obtained in this study.

The conformation corresponding to 210° is calculated to be the most stable for the N_3-protonated species, but the next lowest energy occurs with a torsion angle of 0°. The extra stability for the torsion at 210° may be explained by the formation of a hydrogen bond between the H at N_3 and the oxygen at C_5' (Figure 1). The puckering of the ribose moiety is extremely important for intramolecular hydrogen bonding interactions.[19,25] The difference in energy of the syn (210°) conformation and the anti (0°) conformation for the N_3-protonated species is only 2.29 kcal/mol. These results show that when N_3 is protonated, a larger rotational barrier about the base–ribose bond is present than the rotational barrier for the unprotonated species.

The conformation having the lowest protonation energy occurs with a torsion angle of 330° (Tale IV). The conformation having the next lowest protonation energy occurs for a torsion angle of 210°. As stated earlier, it is quite possible that the stability of this conformation may be due to the formation of a hydrogen bond between the H at N_3 and the O at C_5'. The conformation having the least stable protonation energy occurs for a torsion angle of 150°. In this conformation, the adenine moiety is eclipsed with the C_5' carbon (Figure 4). These results show that N_3-protonation for the anti conformation is more stable than N_3-protonation in the syn conformation by 32.2 kcal/mol. Our results are in excellent agreement with the experimental results[11] obtained from the protonation study of 8-Br-5′AMP and 5′AMP, which indicate that in the syn conformation the N_3 site is not protonated.

(25) (a) Reference 1; Chapter 4. (b) Reference 20.

Our calculations with torsion angles between 60° and 150° failed to converge. These angles correspond to conformations that eclipse the ribose ring (Figure 4). Therefore, it seems that the base does not rotate freely about the ribosyl linkage. The hindered rotation about this bond seems to be due to steric interactions with the ribose ring. In the syn position the sugar equilibrium conformation is only slightly shifted toward the C_2' endo conformation.[19] Since the C_2' endo conformation is the one used for the sugar group in all calculations, and it has been shown that the ribose ring conformation does change with the conformation of the base, this may be a factor involved in causing the calculations at these conformations not to converge.

We were only able to calculate the electronic energies for three conformations of 8-chloroadenosine. The lowest energy conformation occurs with a torsion angle of 210° (Table III, Figure 4). Since the convergence criterion was not met for a larger range of conformations for the 8-Cl-substituted adenosine than for the unsubstituted adenosine, it seems that for nucleotides substituted with bulky substituents at C_8, rotation may be more restricted than for unsubstituted nucleotides.

Conclusions

The localized molecular orbitals from the PRDDO method indicate that the bonding patterns of the double bonds inside the ring of the bases are highly sensitive to the protonated site.

The results for the doubly protonated species indicate that the N_1N_7 doubly protonated species is the most stable, and that the criterion for bonding prescribed by Kleier and Lipscomb for peptides does not hold for charged heterocycles. The transfer of geometries from one basis set to another may also complicate the result.

Our results also show that N_3-protonation for the anti position is more favorable than N_3-protonation in the syn position by 32.2 kcal/mol, which supports the view that steric hinderance inhibits protonation at N_3 for substituted adenine nucleotides and nucleosides that exist predominantly in the syn position. The rotational barrier is higher for N_3-protonated adenine than for unprotonated adenine, and since the most stable conformation for the protonated species is different than the most stable conformation for unprotonated species, a change in conformation may also accompany protonation at N_3. For 8-chloroadenosine, a torsion angle representing the syn conformation (210°) was found to have the lowest energy.

Acknowledgment. We acknowledge support for this work from National Institutes of Health Grant No. RR8006. We thank the Computation Centers of Atlanta University and Atlanta University Center. The figures were prepared with the NIH PROPHET system, a software resource supported by the Division of Resources at the National Institutes of Health. We thank Dr. Henry C. McBay for his helpful comments.

Registry No. I, 73-24-5; AMP, 61-19-8; adenosine, 58-61-7; 8-chloroadenosine, 34408-14-5.